CrossMark

https://doi.org/10.1017/S1551929517000633 Published online by Cambridge University Press

Full Information Acquisition in Scanning Probe Microscopy

S. Jesse, S. Somnath, L. Collins, and S.V. Kalinin*

The Institute for Functional Imaging of Materials and The Center for Nanophase Materials Sciences, Oak Ridge National Laboratory, Oak Ridge, TN 37831

*sergei2@ornl.gov

Abstract: Scanning Probe Microscopy (SPM) has unlocked the nanoworld for exploration and control. While substantial effort has been dedicated toward the development of better instrumental platforms and probes, opportunities related to signal processing and data acquisition in SPM are often overlooked. Here, we discuss opportunities offered by capturing the full information of the data stream from the detector, referred to as General Mode (G-Mode) SPM. This approach allows exploration of the complex tip-surface interactions, spatial mapping of multidimensional variability of material properties and their mutual interactions, and imaging at the information channel capacity limit, providing a new paradigm for SPM detection.

Introduction

Since the invention of atomic force microscopy (AFM) thirty years ago [1], scanning probe microscopies (SPM) have become an enabling technology for nanoscience and technology [2]. The collective effort of commercial, academic, and government institutions have created a fleet of SPM platforms over 50,000 units strong, enabling a broad range of studies from quantum transport imaging in low dimensional systems [3], functional magnetic [4, 5] and ferroelectric studies [6, 7], atomically resolved imaging in ultra-high vacuum (UHV) [8–11] and liquid environments [12], imaging active device structures [13, 14], single molecule reactions [15, 16] , biological recognition imaging [17, 18], and many others. Without exaggeration, SPM has become the key that unlocked the nanoworld for exploration and control.

The original SPMs, including scanning tunneling microscopy (STM) [19, 20] and contact mode atomic force microscopy (AFM) [21], were based on detection of static force or current signals, which imposed severe limitations on the detection limits. Modern dynamic SPMs typically use heterodyne signal processing to amplify weak periodic signals [22]. In this process, they compress the information stream from 10 MHz at the photodetector to ~1–10 kHz, as limited by the rate of the feedback operation and pixel acquisition. In this process the information on transients, non-linear interactions, etc., not captured by the excitations of harmonics, is essentially lost. Correspondingly, a number of groups have suggested approaches based on multiple excitations [23–27], detection of intermodulation signals [26, 28], etc. [29–31]. However, the decoding of this information and its transformation to material-specific properties remains complicated. Furthermore, these complex detection schemes do not provide information on the fundamental question of whether all available information is collected.

Here, we discuss opportunities offered by capturing the full data stream from the detector, referred to as General Mode (G-Mode) SPM. This approach allows exploration of the complex tip-surface interactions, spatial mapping of multidimensional variability of material properties and their mutual interactions, and imaging at the information channel capacity limit—providing a new paradigm for SPM detection. This approach circumvents limitations of heterodyne detection, and as a result unlocks capabilities such as simultaneous multi-resolution imaging at multiple frequencies, smart data compression, noise analysis, and novel spectroscopic methods. In this article, we explore the opportunities for comprehensive materials characterization that are now opened by G-Mode SPM, along with associated instrumental and mathematical challenges. The opportunities enabled by the G-Mode SPM as applied to structural and functional imaging are summarized in Table 1.

Materials and Methods

Signal detection methods. In conventional SPM, a probe with a sharp tip is raster-scanned over the surface while the topography and material properties of the sample are measured by tracking changes in the tip-sample interaction. The vast majority of force-based SPM techniques use a laser-based photodetector system to track changes in the deflection of a cantilever as it interacts with the surface of a sample [32, 33]. Correspondingly, much of the SPM development traditionally targeted the instrument and probe functionality [34]. At the same time, the continuous development of the excitation and signal processing methods is less recognized. In order to achieve a high signal-to-noise ratio, traditional SPM techniques use the

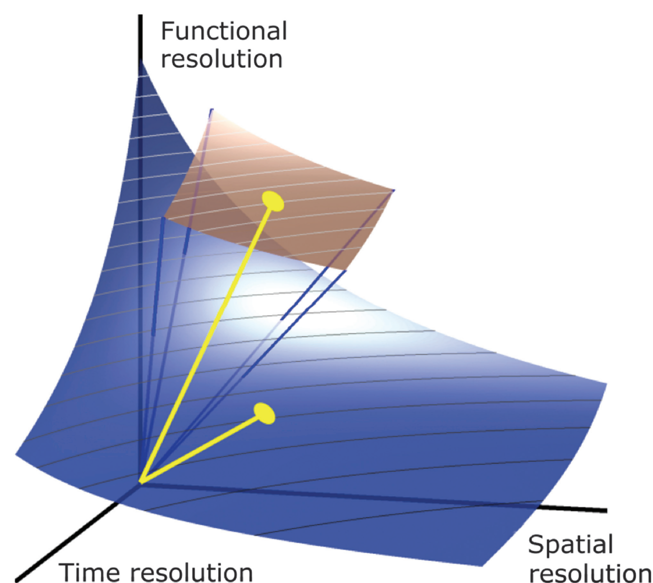

Figure 1: The information in any imaging method can be represented as a combination of the spatial resolution, time resolution, and chemical/functional resolution. Correspondingly, increasing data flow in microscopy can be translated into increased spatial, time, or functional resolution, with the associated conversion factors dependent on technique.

ACCELERATE YOUR *IN SITU* RESEARCH

Whether you are researching new materials or discovering new phenomenon in the electron microscope, nothing should delay your experiment. That's why our service team is always ready to help you with topics ranging from product installation and training to troubleshooting and upgrades. And if you need help with an experiment, we have an applications team with decades of *in situ* experience ready to answer your most challenging questions. We provide all of this for you, because our goal is to accelerate your *in situ* research. Discover more at:

www.protochips.com/contact

Protochips
Quantifiably Better™

https://doi.org/10.1017/S1551929517000633 Published online by Cambridge University Press

https://doi.org/10.1017/S1551929517000633 Published online by Cambridge University Press

dynamic detection principle [35, 36]. In this method, either the probe or the sample is excited mechanically, electrically, magnetically, or thermally using a sinusoidal wave with known frequency, amplitude, and phase. A lock-in amplifier (LIA) isolates the probe response at the driving frequency or its harmonics that are used as the detected signal. Alternatively, phase-locked loops (PLL) are used to maintain the system at resonance by using the phase feedback between excitation and response signal.

Over the last decade it has been recognized that these single-frequency detection methods do not adequately capture the complete information from the tip-surface interactions [25]. This led to the development of multi-frequency SPMs in which the system is excited and measured at two or more frequencies. Passive [37–40], intermodulation [26, 41–44], and feedback-based [29] multi-frequency SPMs have provided considerably deeper insight into the physics of tip-surface interactions in force-based SPMs and have enabled high-resolution imaging and reconstruction of force-distance curves. From passive multi-frequency SPMs, the band excitation (BE) [45, 46] method allowed full characterization of linear tip-surface dynamics. Multi-frequency methods were recently reviewed by Garcia [25].

Information compression. Until recently all dynamic SPM methods universally used the lock-in method of processing to compress the information stream from 10 MHz as limited both by the bandwidth of the photodetector and fundamental physics of the cantilever, to the ~1–10 kHz rate of feedback operation and pixel acquisition. Though these signal streams can be multimodal (for example, intermodulation signals or harmonics), the data flow is still extremely compressed. In the same vein, BE can be represented as a set of parallel lock-ins that compress the data flow to ~100 kHz. Even in this case, the data is compressed to about 1% of the initial data volume. Overall, these approaches restrict the analysis to *a-priori* postulated physical models (for example harmonic response) and ignore information on transients, single events, and incommensurate harmonics appearing in the response. In general, we note there is a direct benefit in increasing the amount of information that can be generated by an imaging tool, as illustrated in Figure 1.

General Mode SPM. In this section we provide an overview of the progress and opportunities for dynamic AFM imaging and analysis based on capturing and analyzing the full data stream from the detector, referred to as General Mode (G-Mode) SPM [47]. The G-Mode SPM concept allows full exploration of complex tip-surface interactions, spatial mapping of multi-dimensional variability of material properties and their mutual interactions, and imaging at the full capacity of the information channel. This approach circumvents limitations of heterodyne detection and, as a result, unlocks capabilities such as simultaneous multi-resolution imaging at multiple frequencies, smart data compression, noise analysis, and spectroscopic methods, which often lead to multiple orders of magnitude improvements in speed compared to classical SPM techniques. Importantly, this approach facilitates the application of a broad set of machine learning tools to the measured responses, thereby taking advantage of existing big data infrastructure and overcoming the limitations imposed by preselected physical model-based analysis [48–50].

Principles of the G-Mode SPM. Figure 2 illustrates the fundamental paradigm of G-Mode SPM, which is the information-theory-based analysis of the full information flow from the detector. The cantilever is driven by a suitably chosen excitation signal corresponding to conventional single frequency, dual frequency, band excitation, or more complex excitation modes. However, unlike the heterodyne or parallel heterodyne processing in the classical and band excitation SPM (BE-SPM), G-Mode SPM captures the full time-dependent response of the cantilever and (temporarily) stores it for the whole image. The raw data is subsequently analyzed and compressed for long-term storage. Multiple information channels such as vertical response, lateral response, and collected current can be captured simultaneously. The stored data are then de-correlated, simplified, and

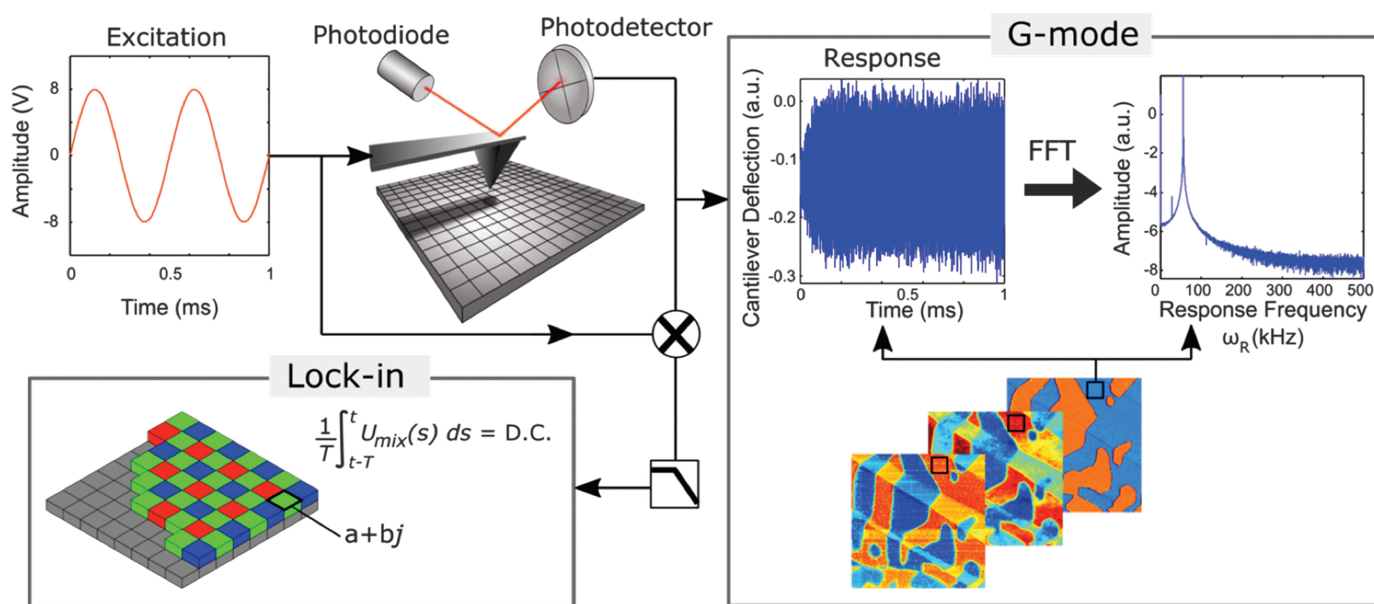

Figure 2: Principles of G-Mode SPM. On the right side, G-Mode captures the complete raw signal from the photodetector thereby adding the time dimension for each spatial pixel. In contrast, the traditional lock-in paradigm (lower left) integrates the product of the excitation and response signals over the time constant and produces a single pair (amplitude and phase) of values at each spatial pixel.

https://doi.org/10.1017/S1551929517000633 Published online by Cambridge University Press

Table 1: Key imaging and spectroscopy modes in scanning probe microscopy (SPM).

Scanning Probe Microscopy Mode	Target Materials / Systems	Significance	Information Provided
Topographic Imaging	All materials and systems	Enabling technique of nanoscience, realized on >50,000 microscope platforms worldwide AFM: ~>80,000 papers with > 1,000,000 citations on Web of Science (ISI)	• Measures surface topography with ~0.1 nm vertical and ~3 nm lateral resolution (contact mode) • Atomic and molecular level resolution possible • Works in an ambient and controlled atmosphere, in liquids, and in vacuum • Phase image (or dissipation) provides information on material composition • Signal recorded on fixed spatial grid
Magnetic Force Microscopy	Magnetic materials	Mainstream tool for magnetic device characterization ~2,800 papers with ~40,000 citations on ISI	• Measures frequency shift and quality factor • Semi-quantitative due to complexity of tip magnetic structure • Sensitive to convolution with stray electrical contrast • Visualization of static magnetic domains with 10–30 nm resolution
Kelvin Probe Force Microscopy	• Semiconductor devices • Photovoltaics • Ferroelectrics • Energy materials • Molecular systems	Mainstream technique for probing electric phenomena on nanometer and atomic level ~1,200 papers with ~18,000 citations on ISI. Developing very rapidly since the past 5 years	• Measures contact potential difference, well defined only for linear dielectric materials • Not suitable in liquids or electrochemical systems • Measurement is static ~10 ms per pixel, no information on local dynamics
Piezoresponse Force / Electrochemical Strain Microscopy	• Ferroelectrics • Piezoelectrics • Biological systems • Memristors • Energy storage and conversion materials	Enabling technique for probing polarization dynamics and ionic transport on the nanoscale PFM: ~1,200 papers with ~19,000 citations; ESM: ~50 papers with ~650 citations on ISI	• Measures electromechanical response of the surface and dissipation • Large number of spectroscopic modes for probing polarization switching
Force Spectroscopy	• Polymer systems • Biological systems • Single molecules • Colloidal solutions	Enabling tool for single-molecule biology, chemistry, and nanomechanics	• Probes local mechanical properties • Provides the structure of double layers and solvation layers in liquids • Single molecule reactions
Current-Voltage Mapping	• Conductors • Semiconductors • Single molecules	Mainstream technique for probing electronic transport properties of samples.	• Correlation of electronic phenomena with topographical features such as grain and phase boundaries • Measurement of local density of states, quasi particle scattering, superconducting gaps

https://doi.org/10.1017/S1551929517000633 Published online by Cambridge University Press

Table 1: Continued.

Scanning Probe Microscopy Mode	Target Materials / Systems	Significance	Information Provided
Emerging Applications: • Multi-frequency imaging (GDM)	• Ferroelectrics and multiferroics • Liquid-based imaging • Polymer systems • Biological systems	Complete understanding of dynamic response. Probes temperature-dependent material properties at the nanoscale	• System response at all frequencies for all excitation frequencies. • Measured quantity is the heat dissipated to the sample • G-Mode can be applied to all SPM modalities

processed using appropriate statistical and physical methods for visualization and interpretation. In this manner, G-Mode is an alternative to lock-in, PLL, or BE detection schemes. Similar to classic detection schemes, measuring the response as a function of local or global stimuli facilitates construction of spectroscopic imaging modes [48, 51].

SPM via G-Mode provides several unique advantages over classical detection schemes that cannot be enabled in other multi-frequency detection schemes. First, the availability of the complete, broadband data stream provides knowledge about the AFM tip-sample interaction for multiple resonance peaks, harmonics, mode mixing, and other non-linear phenomena. Furthermore, the complete data also facilitates adaptive and data-driven signal filtering in the frequency domain instead of using predefined filters as in conventional AFM modes. Second, G-Mode enables multi-resolution imaging, which allows the same data to be represented as a 512 × 512 image with a low noise level or a 512 × 4096 image with higher noise level. This advantage is ideal for measurements requiring precise lateral positioning or imaging of large areas containing small features. Third, G-Mode enables high veracity separation of surface regions with different mechanical, chemical, and electrostatic properties within a single experiment. Below, we illustrate G-Mode implementation for electrostatic force microscopy (EFM), Kelvin probe

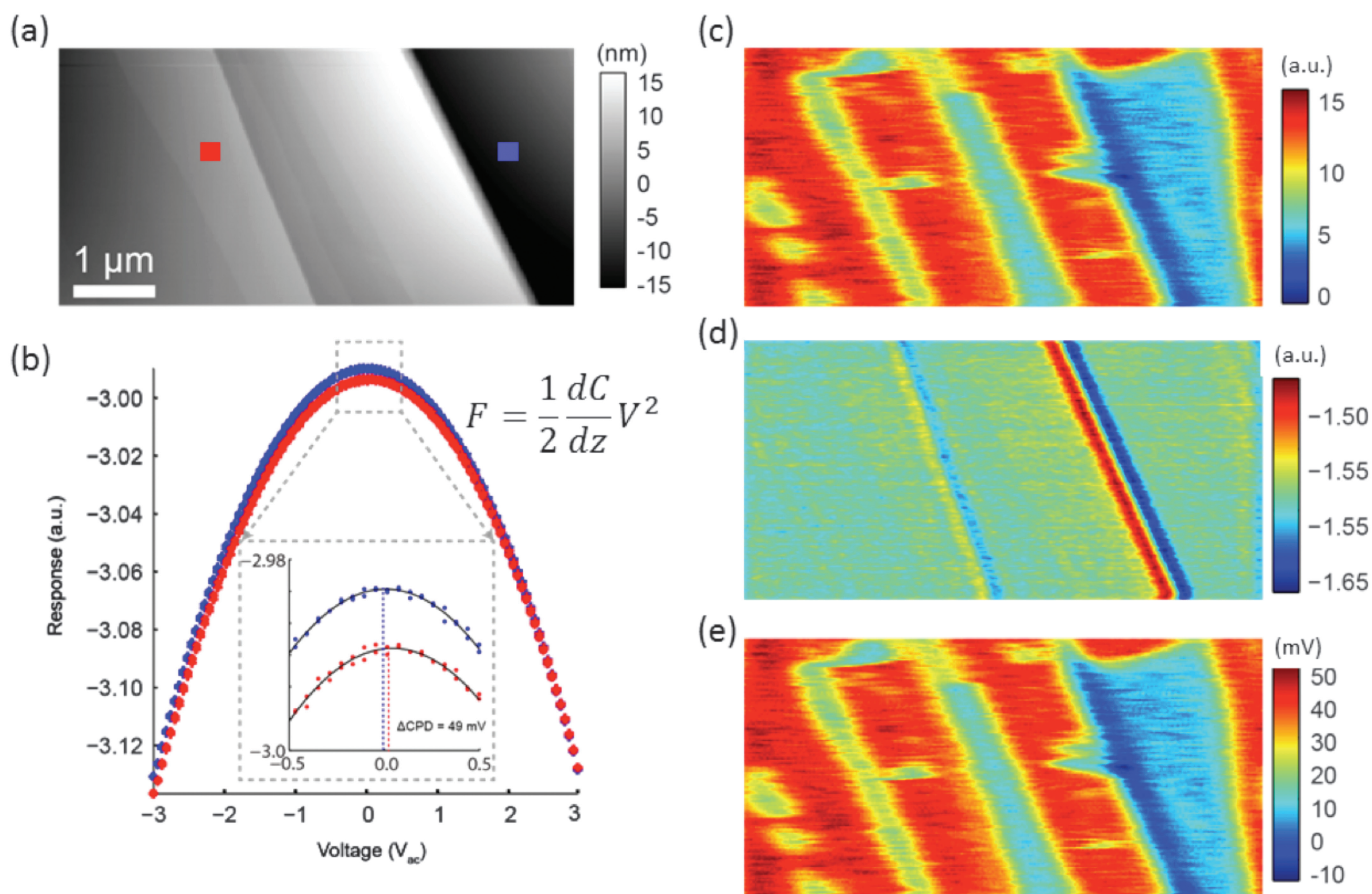

Figure 3: G-Mode KPFM. (a) Topography image of an HOPG sample. (b) Single-point parabolas (averaged over the 4 ms pixel time) for two different locations (indicated via the red and blue squares on (a)) showing a 49 mV offset in the CPD between positions. (c) Second and (d) first order fitting coefficient determined from fitting the parabola at each spatial location for the first period of oscillation. (e) The CPD determined from fitting parameters for the first period of oscillation. Reprinted with permission from L Collins et al., *Scientific Reports* 6 (2016) 30557.

https://doi.org/10.1017/S1551929517000633 Published online by Cambridge University Press

force microscopy (KPFM) [52, 53], and piezoresponse force microscopy (PFM) [54] in the switching and non-switching regimes. For these techniques, we demonstrate physics and information-theory-based analyses, as well as the reduction to classical SPM methods. Finally, we discuss new SPM spectroscopic imaging modalities that are enabled by G-Mode.

Results

Kelvin probe force microscopy. KPFM [55] is an extension of the century-old Kelvin probe technique that allows measurement of the electrochemical or contact potential differences (CPD) between a conductive probe and sample under test. Leveraging the high resolution and force sensitivity of the AFM enables lateral resolution of electronic surface properties on the nanometer [56], and even atomic, scales [57–60]. Classical KPFM uses heterodyne detection and closed-loop-bias feedback to determine the CPD by compensating the potential difference and hence nullifying the electrostatic force between the probe and the sample [55]. This limits the KPFM measurement in terms of channels of information available (that is, CPD is the only channel available) and the time resolution of the measurement (for example, ~1–10 MHz photodetector stream is downsampled to a single readout of CPD per pixel corresponding to ~100 Hz). Furthermore, the feedback loop itself can affect the measurement [61–63].

In contrast, G-Mode KPFM allows the full electrostatic force–bias relationship to be reconstructed with high temporal resolution (~1–3 µs of single cantilever oscillation) for each spatial location of the sample [64, 65]. In G-Mode KPFM, the tip (or sample) only needs the application of an AC voltage, and no bias feedback loop is required. The parabolic dependence of the electrostatic force can be recovered directly by plotting the cantilever response versus the applied voltage as seen in Figure 3. This measurement can be compared with conventional Kelvin probe force spectroscopy (KPFS), in which a linear DC bias sweep is applied to either the tip or the sample, over a single sample location while monitoring the electrostatic force (or force gradient) response using heterodyne detection [66]. This approach avoids many of the complications associated with typical closed-loop KPFM [62] and has even been used to image a single molecular charge under UHV.

In contrast to the KPFS paradigm, which involves long integration times (100 µs to 10 ms) and requires significant amounts of time to collect high-resolution spectroscopic images (for example, several hours) [58], G-Mode KPFM provides the same information, for every oscillation of the AC voltage. In other words, rather than a two-stage detection scheme where an AC response is detected at each voltage of a slow DC waveform, here the force-bias dependence is detected directly. This allows G-Mode KPFM to collect high-resolution maps at regular imaging speeds, as well as retaining high temporal information at every pixel. In Figure 3, the imaging capabilities of G-Mode KPFM are demonstrated on freshly cleaved, highly ordered pyrolytic graphite (HOPG) with a partial delamination of the substrate, exposing graphene layers. The graphene flakes become electronically decoupled from the graphite surface, demonstrating variation in electronic properties across the sample surface. Fitting the bias dependence of the electrostatic force to a second-order polynomial curve, described by $y = ax^2 + bx + c$, is performed to determine several electronic properties including CPD (for exmaple, equal to fitting coefficients $-b/a$) and the capacitance gradient, which is proportional to a.

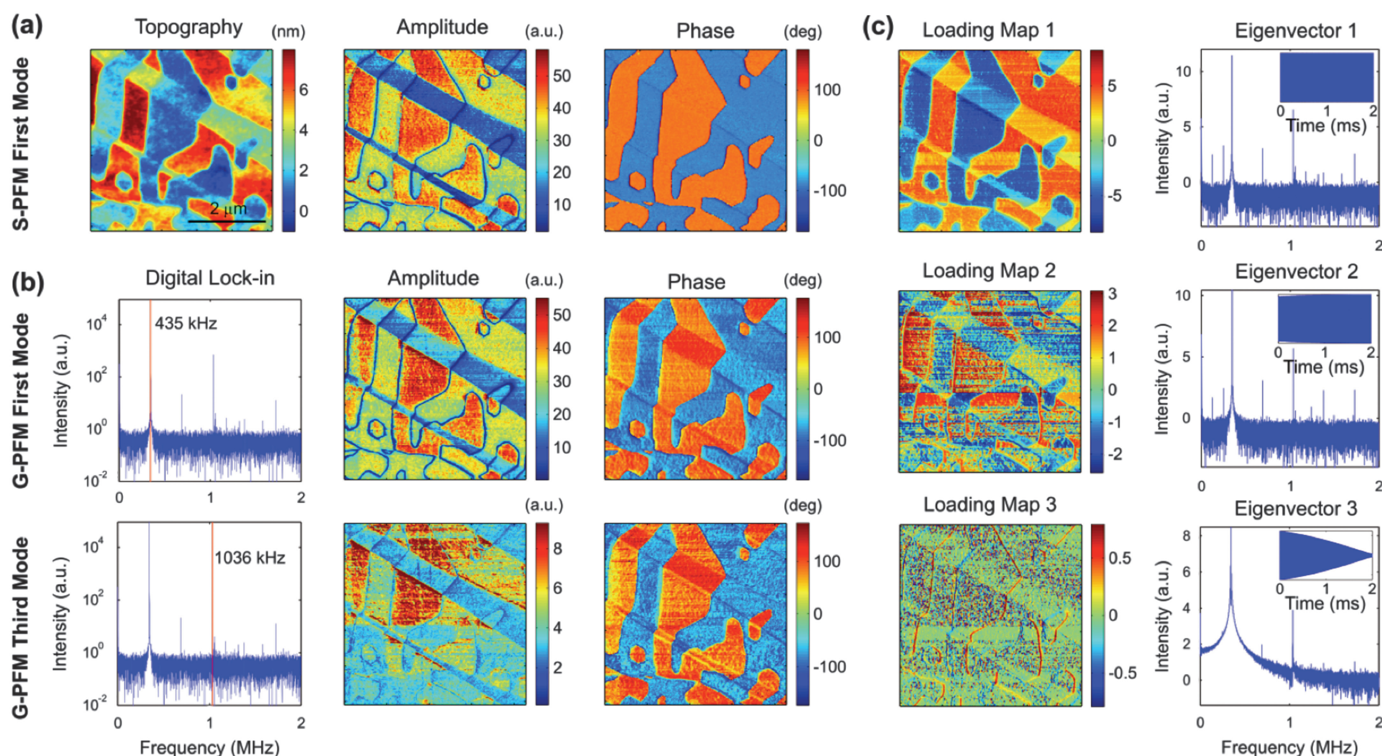

Figure 4: G-Mode PFM imaging. (a) Topography, amplitude, and phase images of a ceramic perovskite obtained from traditional single frequency PFM (S-PFM). (b) Digital lock-ins applied at 435 kHz and 1036 kHz to the G-PFM dataset and the corresponding amplitude and phase maps. (c) Results of principal component analysis (PCA) applied to G-PFM: the first three loading maps and corresponding eigenvectors in frequency-space and real-space (insets). Reprinted from S Somnath et al., *App Phys Lett* 107 (2015) 263102 with permission of AIP Publishing.

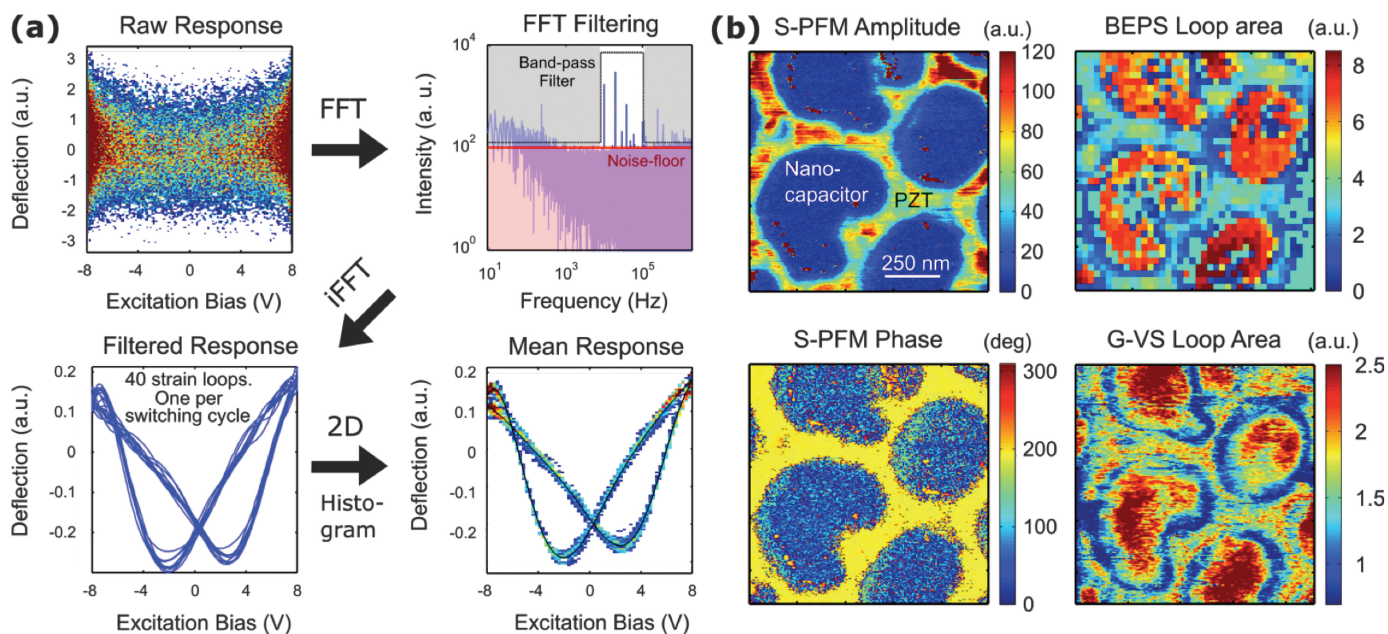

Figure 5: G-Mode voltage spectroscopy (G-VS): a technique for ultrafast imaging of polarization switching in ferroelectric materials. (a) Raw G-VS data filtered in the frequency domain using adaptive noise thresholding and a band-pass filter to reveal multiple material bias-induced strain loops that are characteristic of the hysteretic response shown by ferroelectric materials. (b) Spatial maps of single frequency PFM (S-PFM) amplitude and phase signals, area of the piezoresponse loop from band excitation polarization switching (BEPS), the current state-of-art method for spectroscopic studies on ferroelectric materials, area of the mean strain loops in G-VS. S-PFM and G-VS show high-resolution maps with 256 × 256 spatial pixels acquired in 8.5 and 17 minutes respectively, while BEPS acquired a 40 × 40 pixel image in 77 minutes illustrating that G-VS is 3–4 orders of magnitude faster than BEPS. Reprinted with permission from S Somnath et al., *Nature* Communications 7 (2016) 13290.

Furthermore, G-Mode overcomes the requirement for application of a DC bias [63], which can be problematic for voltage-sensitive materials [67] or operation in liquid [68–70].

It is important to note that despite the popularity of KPFM measurements, the level of information available (that is, CPD) is not sufficient for systems such as electroactive materials, devices, or solid-liquid interfaces, involving nonlinear lossy dielectrics. In such cases it is not enough to know the bias dependence of the electrostatic force (or to be more precise, apex of the parabola); it is imperative that the time dependence of the electrostatic force is also known [70]. In G-Mode KPFM, for every period of AC voltage, the parabolic bias dependence of the electrostatic force, and hence the electronic properties, can be determined [64]. Since the probe raster motion is much slower than the electrical excitation, several 10s–100s of readouts can be performed at each pixel. In this way, G-Mode KPFM provides a measure of the transient changes in electronic properties of the sample at each spatial location, where the temporal resolution of the measurement is on the order of the AC voltage period. This dynamic aspect will be particularly useful for probing surface photovoltage in photovoltaics [71], ion transport in materials and devices [72], and even screening processes at the solid-liquid interface [64]. G-Mode KPFM can potentially enable multi-frequency open-loop KPFM measurements, allow reliable measurements in liquid to probe nonlinear interactions, and improve the measurement rate of KPFM by 1,000 times via direct force-voltage curve reconstructions.

Piezoresponse force microscopy. The PFM technique is used for probing electromechanical activity at the nanoscale and provides insight into localized functionality of ferroelectric and multiferroic materials [6, 73–80]. In PFM, an electric bias is applied to a conductive AFM tip in contact with the sample. The bias results in surface deformation because of the converse piezoelectric effect and/or strain-coupled electrochemical phenomena, as well as an electrostatic force at the tip-surface junction. These surface deformations induce vibrations in the cantilever, which are measured at the AFM photodetector. In spectroscopic modes of PFM, the ferroelectric properties of a material are explored via local hysteresis loop measurements, where the electromechanical response is measured as a function of applied DC bias.

In classical, single-frequency PFM (S-PFM), the cantilever is excited with a sinusoidal bias (typically 10–500 kHz), and the resultant cantilever response is measured using a lock-in amplifier. Consequently, PFM images only contain phase and amplitude information at the excitation frequency at each spatial pixel. In G-Mode PFM (G-PFM) [54] the complete cantilever response at each pixel is stored for later analysis for the same sinusoidal excitation. Similar to KPFM, G-PFM data can be analyzed either by applying digital lock-ins at any frequency or through multivariate statistical analysis methods such as principal component analysis (PCA). Figure 4 compares information from S-PFM, digital lock-in, and PCA applied to an example G-PFM dataset acquired on a polycrystalline $Pb(Zr_{0.2}Ti_{0.8})O_3$ (PZT) ceramic. Here, the loading maps of the first two PCA components show strong contrast between oppositely oriented domains and are similar to the amplitude and phase images from traditional PFM images. Correspondingly, the eigenvectors of the first two components show almost identical harmonic content and correspond to the phase-shifted (by 90 degrees) periodic components of the response. Note that unlike lock-in detection, each PCA component contains multiple harmonics. The third eigenvector is dominated by the intrinsic cantilever resonance,

https://doi.org/10.1017/S1551929517000633 Published online by Cambridge University Press

EXPLORE THE HIGHEST RESOLUTION
EXPLORE THE POSSIBILITIES
EXPLORE S8000 series

S8000
NEW FAMILY OF TESCAN MICROSCOPES

ULTRA-FAST CROSS-SECTIONS AND 3D ANALYSIS

DAMAGE-FREE ULTRATHIN SAMPLE PREPARATION

VISIT US AT BOOTH
No. 1508 AT M&M 2017

Stop by to learn more about the very new generation of tools offered by TESCAN.

https://doi.org/10.1017/S1551929517000633 Published online by Cambridge University Press

https://doi.org/10.1017/S1551929517000633 Published online by Cambridge University Press

Table 2: G-Mode Limitations

Problem or Limitation	Solution/Comment
Large data volumes: classical 2D SPM image is 1 MB, an equivalent full G-Mode image is 4 GB	• Compression with minimal information loss reduces the data volume to ~40 MB depending on information content in data. • Due to the emergence of cloud storage and high-density disk arrays, storage has become a much smaller issue, even in comparison to the scenario 5 years ago; this is a trend that is expected to continue in the future. • Information captured in G-Mode is simply inaccessible using classical methods, making the technique worthwhile. • Lossless compression allows full reconstruction of signal for continuous analysis with a wide variety of methods. • Sparse methodology using intrinsic data structure provides a pathway to a much higher degree of compression than currently available.
Information theory methods such as PCA ignore relevant physics and hence can be difficult to interpret	• Physics-based compression methods (lossy compression) have been demonstrated in other communities and can be adapted for SPM dynamics. • More robust Bayesian inference, as well as supervised learning methods with built-in physical constraints, are available to analyze G-Mode data.
No current feedback system in G-Mode: precludes realization of frequency-tracking modes	• Presently, feedback can be run in parallel to classical SPM processing. • Fast FPGA processing will allow real-time feedback. The tools are available and are being implemented in next iterations of the G-Mode techniques.
Information overload: full cantilever trajectory as a function of force or voltage excitation often contains many more components than are captured by classical methods, overloading the user	• This information is relevant to material behavior and is rooted in real phenomena that is otherwise lost or ignored. • Broad-based theory support is developing a mathematical framework for extracting material properties from probe trajectories, mixed harmonic signals, etc. However, these are generally limited due to the novelty of the technique. • Synergy with the global open-source software development community (for example, through GitHub distribution) will allow effective deployment and a dialogue in the scientific community.
Serendipitous phenomena: transients, single events, etc. complicate true material behavior reconstruction	• Information without clear interpretation can always be analyzed as new theories are developed. • G-Mode can always be reduced to classical methodology of lock-in, or Band Excitation techniques. • Practically, this new technique can elucidate material behavior coupling, or help characterize the measuring tool itself, decoupling real physical properties from instrumentation bias.

and the corresponding loading map shows characteristics of the transient cantilever response induced by the edges of topographical features, resembling the error signal in the force feedback loop. Appropriate signal de-mixing algorithms can be used to decouple domain contrast from topographic information. These G-PFM data can also be analyzed using clustering algorithms, independent component analysis, Bayesian linear unmixing methods, and correlational analysis techniques [48, 81–86].

The G-PFM approach can also be extended to study polarization switching in ferroelectric materials, as implemented in G-Mode voltage spectroscopy (G-VS) [87]. In G-VS, the amplitude of the G-PFM excitation signal is increased beyond the coercive bias of the sample. G-VS uses data-driven adaptive signal filtering techniques to reveal strain loops that are indicative of polarization switching in ferroelectric materials, as shown in Figure 5a. The raw data itself is used to calculate an appropriate noise-floor for the signal at each pixel. A band-pass filter only retains the signal from the excitation frequency to 10–12 harmonics of the drive frequency, and any signal below the calculated noise floor is rejected. The filtered signal reveals numerous bias-induced strain loops. Such extraction of hysteresis loops would not be possible without the complete data or by using the traditional heterodyne detection schemes since the response frequencies are not known *a priori*. Compared to the current state-of-art

https://doi.org/10.1017/S1551929517000633 Published online by Cambridge University Press

technique, band excitation polarization switching (BEPS) that uses a slow (0.25–2 Hz) polarization switching waveform, the ultrafast excitation waveform of G-VS (10–60 kHz) results in a 3,500-fold improvement in measurement speed over BEPS. The sheer speed of the polarization switching waveform enables G-VS to enjoy high spatial resolution, minimal drift, and short measurement durations typical of imaging modes such as S-PFM, while having the polarization switching capability of spectroscopy techniques. Once the data are filtered, relevant material-specific properties may be extracted from the shape of the strain loops. Alternatively, statistical methods may be applied to analyze the data. Figure 5b compares the spatial resolutions of S-PFM, BEPS, and G-VS for measurements on a $Pb(Zr_{0.2}Ti_{0.8})O_3$ (PZT) thin film sandwiched between gold nanocapacitor discs and a $SrRuO_3$ bottom electrode on a $SrTiO_3$ substrate. The S-PFM and G-VS measurements resulted in high-resolution 256 × 256 pixel images acquired in 8.5 and 17 minutes, respectively, while the BEPS measurement resulted in a 40 × 40 pixel image acquired in 77 minutes.

New SPM modes enabled by full data acquisition. Besides adaptations to traditional imaging techniques, G-Mode also can give rise to fundamentally new modes of SPM operation [88]. For example, in order to completely characterize any system,

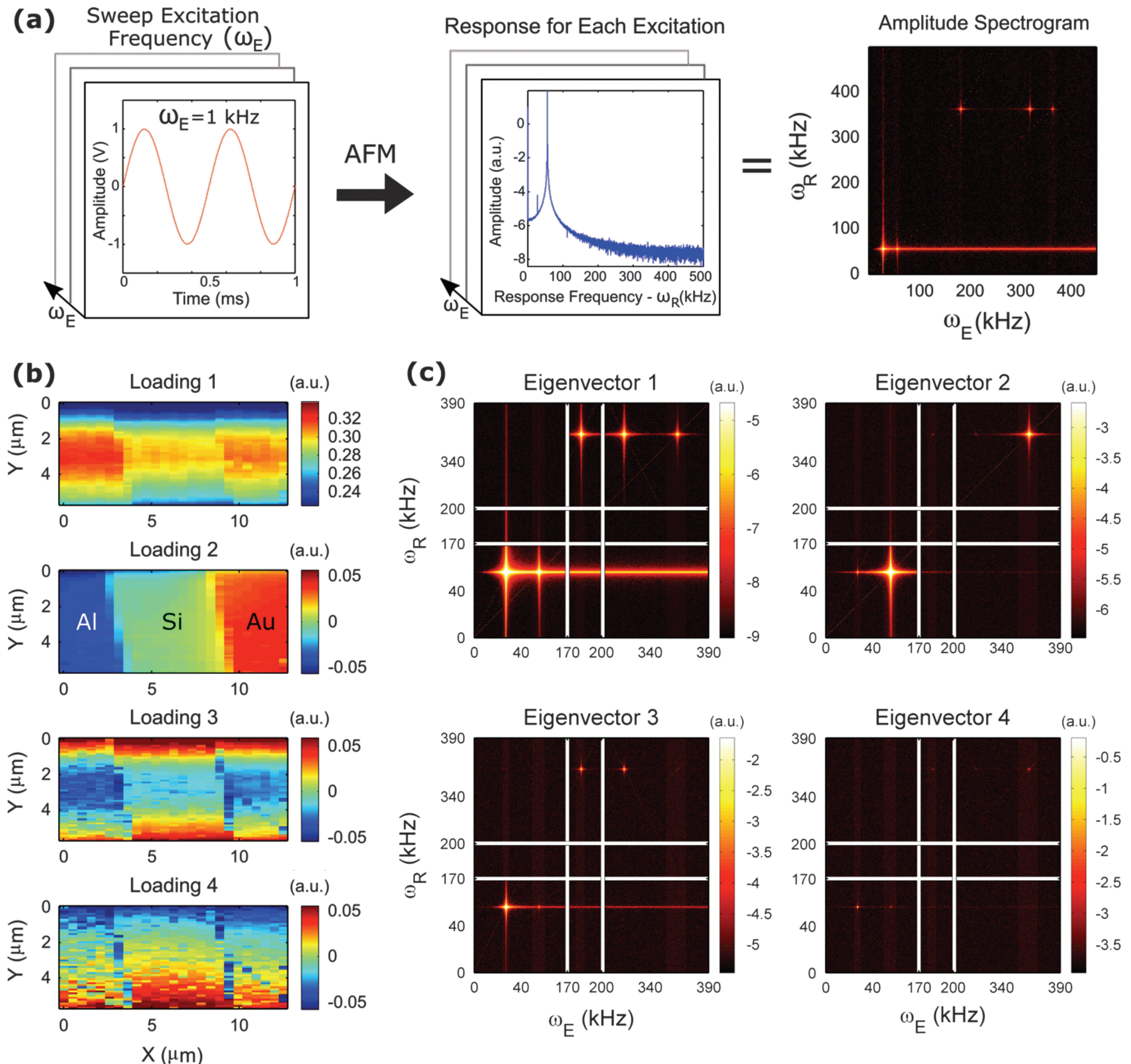

Figure 6: General dynamic mode (GDM) applies G-Mode to frequency sweeps. (a) In GDM, the complete response from the AFM is recorded for a sequence of excitation waveforms of increasing frequency to generate a 2D spectrogram with the excitation frequency on one axis and the response frequency on the other for each spatial location. (b-c) Results of PCA applied to a GDM imaging dataset on a silicon substrate with gold and aluminum electrodes. The first four PCA loading maps (b) and eigenvectors (c), which are GDM spectrograms. Reprinted from S Somnath et al., *Nanotechnology* 27 (2016) 414003 with permission of IOP Publishing.

https://doi.org/10.1017/S1551929517000633 Published online by Cambridge University Press

it is important to study the dynamic behavior of the system to identify and isolate the contributions of different phenomena with respect to the system's response.

Figure 6a illustrates general dynamic mode (GDM), which applies the G-Mode methodology to frequency sweeps such that the result at each spatial location is a two-dimensional dataset with excitation frequency (ω_E) on one axis and the response frequency (ω_R) on the other. GDM can be extended to imaging on a grid of points or spectroscopic measurements, where one or more system parameters are varied, to generate datasets with 3 or more dimensions and data sizes that can range from 10 GB to 1000 GB. Such GDM spectroscopic or imaging datasets can be analyzed using PCA or established physical models.

Figures 6b and 6c illustrate the results from PCA applied to a four-dimensional (x, y, ω_E, ω_R) GDM imaging dataset acquired for a model system of a purely capacitively actuated cantilever over a silicon sample with gold and aluminum electrodes. The Eigenvectors from PCA are GDM spectrograms that show prominent peaks at the first two resonant modes of the cantilever as well as their first harmonic. The first PCA component shows the mean response over the entire dataset. The eigenvector from the second component is dominated by response from the resonance peaks, and the corresponding loading map shows a distinct response from each phase in the sample. The third component resembles the capacitance gradient, which is dependent on the dielectric properties of the sample and the tip-surface geometry. The loading map from the fourth component appears to be sensitive to the topography edges only, and the subsequent PCA components mainly contain noise. GDM reveals vital information such as mode-mixing, harmonics, and other non-linear behaviors of systems that are impossible to visualize using other techniques [88]. GDM could also be applied to measurements such as contact resonance to extract more information about the viscoelastic properties of materials.

In addition, G-Mode also can be applied to other SPM modes such as magnetic force microscopy (MFM) [53] and intermittent contact mode imaging [47], in many cases offering several orders of magnitude greater speed in imaging. Since G-Mode captures several data points for each oscillation of the AFM cantilever, force-distance curves can be extracted from G-Mode intermittent contact mode measurements to enable rapid acquisition of dense 3D grids of the tip-sample forces. Much like G-VS, these measurements would be at least 3 orders of magnitude faster than classical force-mapping measurements that use heterodyne detection methods. However, the key challenge is the inversion of data to extract the force-distance curves. Similarly, applying G-Mode to current-voltage (IV) measurements can decrease measurement time by 2–3 orders of magnitude and facilitate the capturing of materials physics that is not possible with conventional methods. Yet again, the inversion of data to extract the local resistance as a function voltage via methods such as Bayesian inference will be a challenge. In addition, G-Mode applied to MFM enables the measurement of magnetic domains, average dissipation, and single dissipation events from a single experiment. Furthermore, it is possible to deconvolute electronic effects, and probe the non-linearities and frequency-dependent mixing phenomena in G-Mode MFM.

Discussion

The (temporary) capture of the complete information stream and subsequent analysis requires advanced computational capabilities, as summarized in Table II. However, the explosive growth of cloud-enabled computing technologies makes these calculations highly feasible [48–50]

The potential of G-Mode SPM to attain the ultimate goal for an SPM experiment, that is, quantitative probing of local material functionality, has two stages, namely reconstruction of the force-distance (FD) curve (for dynamic measurements) or force-voltage curve (for voltage modulated measurements) from the measured signals and the physics-based analysis to extract local functionalities. Indeed, the FD curves contain the full information about the tip-surface interactions and represent the maximum amount we can extract from SPM measurements without additional information on the tip-geometry and properties. Correspondingly, the next step of G-Mode SPM is the introduction of mathematical frameworks and modulation modes that allow reconstruction of local FD curves from the dynamic data. Once available, this will open a pathway for physics-based analysis. Furthermore, the linearity of FD interactions in terms of relevant contributions suggests a tremendous potential for blind linear unmixing methods to separate local contributions, giving rise to new SPM imaging paradigms.

Conclusion

This article describes a new scanning probe microscopy method called General Mode (G-Mode) SPM, which allows exploration of the entire signal resulting from complex tip-surface interactions. Typical G-Mode SPM allows spatial mapping of the multi-dimensional variability in material properties and their interactions on a pixel-by-pixel basis. Imaging and spectroscopy with this method uses the entire capacity of the available information channels.

Acknowledgements

This research was funded by the Center for Nanophase Materials Sciences, which is a U. S. Department of Energy Office of Science User Facility.

References

[1] G Binnig et al., *Phys Rev Lett* 56(9) (1986) 930.
[2] C Gerber and HP Lang, *Nat Nanotechnology* 1(1) (2006) 3–5.
[3] MA Topinka et al., *Nature* 410(6825) (2001) 183–6.
[4] Y Martin and HK Wickramasinghe, *Appl Phys Lett* 50(20) (1987) 1455–57.
[5] P Grutter et al., *Appl Phys Lett* 71(2) (1997) 279–81.
[6] DA Bonnell et al., *MRS Bull* 34(9) (2009) 648–657.
[7] SV Kalinin et al., *Rep Prog Phys* 73(5) (2010) 056502.
[8] G Binnig et al., "7 × 7 Reconstruction on Si(111) Resolved in Real Space" in *Scanning Tunneling Microscopy* ed. H Neddermeyer, Springer, New York, (1993) 36–39.
[9] G Binnig et al., *Europhys Lett* 3(12) (1987) 1281.
[10] TR Albrecht and C Quate, *J Appl Phys* 62(7) (1987) 2599–02.
[11] FJ Giessibl, *Mater Today* 8(5) (2005) 32–41.
[12] T Fukuma et al., *Appl Phys Lett* 87(3) (2005) 034101.
[13] M Tanimoto and O Vatel, *J Vac Sci Technol B* 14(2) (1996) 1547–51.

https://doi.org/10.1017/S1551929517000633 Published online by Cambridge University Press

[14] BD Huey and DA Bonnell, *Appl Phys Lett* 76(8) (2000) 1012–14.
[15] H Clausen-Schaumann et al., *Curr Opin Chem Biol* 4(5) (2000) 524–30.
[16] M Rief et al., *Science* 275(5304) 1997) 1295–97.
[17] P Hinterdorfer and YF Dufrene, *Nat Methods* 3(5) (2006) 347–55.
[18] C Stroh et al., *P Natl Acad Sci USA* 101(34) (2004) 12503–07.
[19] G Binnig and H Rohrer, *Helv Phys Acta* 55(6) (1982) 726–35.
[20] G Binnig et al., *Phys Rev Lett* 50(2) (1983) 120–23.
[21] G Binnig et al., *Phys Rev Lett* 56(9) (1986) 930–33.
[22] R Garcia and R Perez, *Surf Sci Rep* 47(6–8) (2002) 197–301.
[23] TR Rodrıguez and R García, *Appl Phys Lett* 84(3) (2004) 449–51.
[24] N Martinez et al., *Nanotechnology* 19(38) (2008) 384011.
[25] R Garcia and ET Herruzo, *Nat Nanotechnol* 7(4) (2012) 217–26.
[26] D Platz et al., *Appl Phys Lett* 92(15) (2008) 153106.
[27] RW Stark et al., *Phys Rev B* 69(8) (2004) 085412.
[28] D Platz et al., *Nanotechnology* 23(26) (2012) 265705.
[29] BJ Rodriguez et al., *Nanotechnology* 18(47) (2007) 475504.
[30] DS Santiago and C Gaurav, *Meas Sci Technol* 21(12) (2010) 125502.
[31] O Sahin et al., *Nat Nanotechnol* 2(8) (2007) 507–514.
[32] G Meyer and NM Amer, *Appl Phys Lett* 56(21) (1990) 2100–01.
[33] CA Putman et al., *J Appl Phys* 72(1) (1992) 6–12.
[34] CCM Mody, *Instrumental community: Probe microscopy and the path to nanotechnology*. MIT Press, Cambridge, MA, 2011.
[35] S-i Kitamura and M Iwatsuki, *Jpn J Appl Phys* 34(1B) (1995) L145.
[36] FJ Giessibl, *Science* 267(5194) (1995) 68–71.
[37] JR Lozano and R Garcia, *Phys Rev Lett* 100(7) (2008) 076102.
[38] D Martinez-Martin et al., *Phys Rev Lett* 106(19) (2011) 198101.
[39] G Chawla and SD Solares, *Appl Phys Lett* 99(7) (2011) 074103.
[40] SD Solares and G Chawla, *Meas Sci Technol* 21(12) (2010) 125502.
[41] D Forchheimer et al., *Phys Rev B* 85(19) (2012) 195449.
[42] D Platz et al., *Ultramicroscopy* 110(6) (2010) 573–77.
[43] SS Borysov et al., *Phys Rev B* 88(11) (2013) 115405.
[44] EA Tholén et al., *Rev Sci Instrum* 82(2) (2011) 026109.
[45] S Jesse et al., *Nanotechnology* 18(43) (2007) 435503.
[46] S Jesse and SV Kalinin, *J Phys D-Appl Phys* 44(46) (2011) 464006.
[47] A Belianinov et al., *Nature Communications* 6 (2015), article no. 7801.
[48] A Belianinov et al., *Adv Struct Chem Imag* 1(1) (2015) 1–25 (2015).
[49] EJ Lingerfelt et al., *Procedia Computer Science* 80 (2016) 2276–80.
[50] SV Kalinin et al., *ACS Nano* 10(10) (2016) 9068–86.
[51] RK Vasudevan et al., *MRS Commun* 2(3) (2012) 61–73.
[52] L Collins et al., *Nanotechnology* 27(10) (2016) 105706.
[53] L Collins et al., *Appl Phys Lett* 108(19) (2016) 193103.
[54] S Somnath et al., *Appl Phys Lett* 107(26) (2015) 263102.
[55] M Nonnenmacher et al., *Appl Phys Lett* 58(25) (1991) 2921–23.
[56] U Zerweck et al., *Phys Rev B* 71(12) (2005) 125424.
[57] L Gross et al., *Science* 324(5933) (2009) 1428–31.
[58] F Mohn et al., *Nat Nanotechnol* 7(4) (2012) 227–31.
[59] K Okamoto et al., *Appl Surf Sci* 210(1) (2003) 128–33.
[60] F Bocquet et al., *Phys Rev B* 78(3) (2008) 035410.
[61] SV Kalinin and DA Bonnell, *Phys Rev B* 63(12) (2001) 125411.
[62] L Collins et al., *Nanotechnology* 24(47) (2013) 475702.
[63] K Okamoto et al., *Appl Surf Sci* 188(3–4) (2002) 381–85.
[64] L Collins et al., *Scientific Reports* 6 (2016) 30557.
[65] L Collins et al., *Nanotechnology* 27(10) (2016) 105706.
[66] L Collins et al., *Appl Phys Lett* 106(10) (2015) 104102.
[67] S Yoshida et al., e-Journal of *Surface Science and Nanotechnology* 4(0) (2006) 192–96.
[68] L Collins et al., *Appl Phys Lett* 104(13) (2014) 133103.
[69] L Collins et al., *Nat Commun* 5 (2014), article no. 5293.
[70] L Collins et al., *Beilstein Journal of Nanotechnology* 6(1) (2015) 201–14.
[71] DC Coffey and DS Ginger, *Nat Mater* 5(9) (2006) 735–40.
[72] E Strelcov et al., *ACS Nano* 7(8) (2013) 6806–15.
[73] A Gruverman et al., *Annu Rev Mater Sci* 28 (1998) 101–23.
[74] A Gruverman et al., *Nanotechnology* 8 (1997) A38–A43.
[75] N Balke et al., *J Am Ceram Soc* 92(8) (2009) 1629–47.
[76] SV Kalinin et al., *MRS Bulletin* 34(9) (2009) 634–42.
[77] SV Kalinin et al., *IEEE T Ultrason Ferr* 53(12) (2006) 2226–52.
[78] NA Polomoff et al., *J Mat Sci* 44(19) (2009) 5189–96.
[79] C Dehoff et al., *Rev Sci Instrum* 76(2) (2005) 02378.
[80] CS Ganpule et al., *Appl Phys Lett* 77(2) (2000) 292–94.
[81] A Halimi et al., *IEEE Trans Image Process* 24(12) (2015) 4904–17.
[82] N Bonnet. Artificial intelligence and pattern recognition techniques in microscope image processing and analysis. in *Advances in Imaging and Electron Physics* Vol 114. ed PW Hawkes, Elsevier Academic Press Inc, San Diego, (2000) 1–77.
[83] N Bonnet, *J Microsc-Oxf* 190 (1998) 2–18.
[84] O Eches et al., *IEEE Trans Image Process* 22(1) (2013) 5–16.
[85] Y Altmann et al., *IEEE Trans Signal Process* 61(10) (2013) 2442–53.
[86] N Dobigeon and N Brun, *Ultramicroscopy* 120 (2012) 25–34.
[87] S Somnath et al., *Nat Commun* 7(2016) 13290.
[88] S Somnath et al., *Nanotechnology* 27(41) (2016) 414003.

MT